

DIAGNOSING THE OUTFLOW FROM THE SGR 1806-20 GIANT FLARE WITH RADIO OBSERVATIONS

J. GRANOT¹, E. RAMIREZ-RUIZ², G. B. TAYLOR^{1,3}, D. EICHLER⁴, Y. E. LYUBARSKY⁴, R. A. M. J. WIJERS⁵, B. M. GAENSLER⁶,
R. P. FENDER⁷, J. D. GELFAND⁶, C. KOUVELIOTOU⁸, P. M. WOODS⁹

Draft version March 14, 2005

ABSTRACT

On 2004 Dec. 27, the soft gamma repeater (SGR) 1806-20 emitted the brightest giant flare (GF) ever detected from an SGR. This burst of energy, which resulted in an (isotropic) energy release ~ 100 times greater than the only two other known SGR GFs, was followed by a very bright, fading radio afterglow. Extensive follow-up radio observations provided a wealth of information with unprecedented astrometric precision, revealing the temporal evolution of the source size, along with densely sampled light curves and spectra. Here we expand on our previous work on this source, by attempting to explain these observations within one self-consistent dynamical model. In this scenario, the early radio emission is due to the outflow ejected during the GF energizing a thin shell surrounding a pre-existing cavity, where the observed steep temporal decay is attributed to the adiabatic cooling of the electrons in the doubly shocked medium. The shocked ejecta and external shell move outward together, driving a forward shock into the ambient medium, and are eventually decelerated by a reverse shock. The radio emission from the shocked external medium naturally peaks when significant deceleration occurs, and then decays relatively slowly. The evolution of the source size is reproduced in our model, and suggests that most of the energy in the outflow was in mildly relativistic material, with $v/c \sim 0.4d_{15}$, for a distance of $15d_{15}$ kpc to SGR 1806-20. An initially highly relativistic outflow would not have produced a long coasting phase at a mildly relativistic expansion velocity, as was observed.

Subject headings: stars: neutron – stars: flare – stars: winds, outflows – hydrodynamics – ISM: bubbles

1. INTRODUCTION

Soft gamma repeaters (SGRs) are believed to be “magnetars” – a small class of slowly spinning neutron stars with extremely high surface magnetic fields, $B \sim 10^{15}$ G (Duncan & Thompson 1992; Kouveliotou et al. 1998). SGR 1806-20 lies in the Galactic plane, at a distance of about $d = 15d_{15}$ kpc (Corbel & Eikenberry 2004). The giant flare (GF) from SGR 1806-20 on 2004 Dec. 27, was the brightest extra-solar transient event ever recorded (Hurley et al. 2005; Palmer et al. 2005). It was also unique in its bright radio afterglow (Cameron & Kulkarni 2005; Gaensler et al. 2005) which provided an amazing variety of data, including the source size, shape, polarization and flux at different radio frequencies as a function of time.

In an accompanying paper (Gelfand et al. 2005), we have presented a rebrightening episode in the radio light curve, and have developed a semi-analytic model for the radio source that appeared in the aftermath of the giant flare. We concluded from a fit of this model to the data that the radio source resulted from a blast wave driven by $\gtrsim 10^{24.5}$ g of baryonic material driven off the neutron star, and that this source has now entered the Sedov-Taylor phase of evolution. On-going measurements of the evolution of the source’s size confirm that the radio source is decelerating (Taylor et al. 2005, in prep.).

These data present a rare opportunity for a detailed study of an outflow that is at least mildly relativistic, and which has many similarities to cosmological gamma-ray bursts. In this *Letter*, we expand on the framework laid out by Gaensler et al. (2005) and Gelfand et al. (2005), presenting a full dynamical model for the interaction of the outflow that was ejected in the Dec. 27 GF with its surroundings, with a view to explaining the large and diverse data for this event. This enables us to constrain the initial velocity for this outflow.

Our model is described and analyzed in §2. We consider both a relativistic (§2.1) and a Newtonian (§2.2) outflow, and find that only a Newtonian outflow with $v/c \sim 0.4d_{15}$ works well.¹⁰ This scenario is studied in detail using hydrodynamic simulations (§2; Fig. 1), and compares well with the data. In §3 the synchrotron emission that is implied by our dynamical model is derived and shown to nicely agree with observations. Our conclusions are discussed in §4.

2. THE UNDERLYING DYNAMICS

The radio flux was initially observed to decay with time, exhibiting an achromatic steepening (to $\sim t^{-2.7}$) at $t_b \approx 9$ days (Gaensler et al. 2005). This was followed by a rebrightening starting at ~ 25 days and peaking at ~ 33 days (Gelfand et al. 2005), and then showed a slower decay ($\sim t^{-1.3}$). The expansion velocity was initially fairly constant, $\sim 0.4d_{15}c$ (see footnote 10), and later decreased, around the peak time of the rebrightening in the light curve (Taylor et al. 2005, in prep.). The source was already fading by the time of the first observation, $t_1 \approx 7$ days. This implies that the radio emission must have turned on at an earlier time and at a smaller radius.

The observed spectrum and linear polarization suggest that we are seeing synchrotron emission. If the relativistic electrons that are emitting this radiation were accelerated much

¹ KIPAC, Stanford University, P.O. Box 20450, MS 29, Stanford, CA 94309; granot@slac.stanford.edu

² IAS, Einstein Drive, Princeton, NJ 08540; Chandra Fellow

³ NRAO, P.O. Box O, Socorro, NM 87801

⁴ Dept. of Phys., BGU, P.O. Box 653, Be’er Sheva 84105, Israel

⁵ Astronomical Institute “Anton Pannekoek”, University of Amsterdam, Kruislaan 403, 1098 SJ, Amsterdam, The Netherlands

⁶ Harvard-Smithsonian Center for Astrophysics, 60 Garden Street, Cambridge, MA 02138

⁷ School of Physics and Astronomy, University of Southampton, Highfield, Southampton SO17 1BJ, UK

⁸ NASA/MSFC, NSSTC, 320 Sparkman Dr., Huntsville, AL 35805

⁹ USRA, NSSTC, 320 Sparkman Dr., Huntsville, AL 35805

¹⁰ We adopt the value that was derived by Taylor et al. (2005, in prep.) for the average expansion velocity during the first month so. It is slightly higher than the value reported initially by Gaensler et al. (2005).

closer to the source, then most of their energy would have been lost through adiabatic cooling by t_1 , thus dramatically increasing the energy requirements. Moreover, the light curve showed a dramatic achromatic steepening at t_b (Gaensler et al. 2005), which suggests a hydrodynamic transition. A simple explanation for this behavior arises if the outflow from the GF initially coasted with negligible interaction with the ambient medium, until at $t_{\text{col}} = 5t_{\text{col},5}$ days it collided with a thin shell, which caused it to decelerate by a reverse shock, while the external shell was accelerated by a forward shock.¹¹ After this collision the two shells move together (at a somewhat reduced speed). The emission up to t_b is dominated by the recently shocked electrons in these two shells. It arrives at the observer at a time $t \lesssim (1.5-2)t_{\text{col}}$ due to light travel effects and the finite time it takes the shock to cross the shells. At $t > t_b$ the emission is dominated by the adiabatically cooling electrons in the two shells. As shown below (see also Gaensler et al. 2005) this naturally produces the observed steep decay.

As the merged shell expands outwards it drives a shock into the ambient medium. An increasing amount of external mass is swept up, until the emission from this shocked fluid starts dominating the light curve at $t \gtrsim 25$ days. This causes a re-brightening in the light curve which peaks at $t_p \sim 33$ days (Gelfand et al. 2005); a decrease in the expansion velocity was observed at about the same time, $t_{\text{dec}} \sim t_p$ (Taylor et al. 2005, in prep.), as expected. At $t > t_{\text{dec}}$ the hydrodynamics gradually approach the self similar Sedov-Taylor solution, which predicts a slower flux decay rate, in agreement with observations (Gelfand et al. 2005). In the following we reproduce the main observed features using a simple analytic model, and then compare it to the results of numerical simulations.

2.1. Relativistic Outflow

A simple model for the collision between the cold ejecta shell of initial Lorentz factor $\Gamma_0 = (1 - \beta_0^2)^{-1/2}$ and mass M_0 , and an external shell (at rest) of mass M_{sh} , is a plastic collision where the two shells are shocked (the two shocked fluids separated by a contact discontinuity) and subsequently move together at $\Gamma_f = (1 - \beta_f^2)^{-1/2}$. Energy and momentum conservation in the rest frame of the merged shell are $E_f/c^2 = M_f = \Gamma_r M_0 + \Gamma_f M_{\text{sh}}$ and $\Gamma_r \beta_r M_0 = \Gamma_f \beta_f M_{\text{sh}}$, respectively, where $\Gamma_r = (1 - \beta_r^2)^{-1/2} = \Gamma_0 \Gamma_f (1 - \beta_0 \beta_f)$ is the initial Lorentz factor of the ejecta in this frame. The resulting internal energy is $E_{\text{int}}/c^2 = (\Gamma_r - 1)M_0 + (\Gamma_f - 1)M_{\text{sh}}$ and the final velocity is

$$\frac{\beta_f}{\beta_0} = \left(1 + \frac{M_{\text{sh}}}{\Gamma_0 M_0}\right)^{-1}. \quad (1)$$

This shows that an external mass of $M_{\text{sh}} \sim \Gamma_0 M_0$ is required in order to significantly reduce the initial velocity. For a relativistic outflow $\Gamma_0 \approx E/M_0 c^2 \gg 1$ and $\beta_0 \approx 1$ so that $\beta_f \approx (1 + M_{\text{sh}} c^2/E)^{-1}$ which for $M_{\text{sh}} c^2 \gg E$ (and correspondingly $\beta_f \ll 1$) gives $M_{\text{sh}} v_f^2 \approx \beta_f E$. Therefore, in this limit, the kinetic energy of the merged shell carries only a small fraction

¹¹ Such a shell surrounding a pre-existing cavity is thought to be formed behind the bow shock due to the supersonic motion of SGR 1806-20 through the ISM and its quiescent wind (Gaensler et al. 2005). Alternatively, it could also arise from an earlier and initially faster mass ejection from the SGR 1806-20 GF, which was decelerated by the external medium to a velocity slightly below that of the coasting second shell, thus causing the two shells to collide (the “refreshed shock” scenario, e.g. Granot, Nakar & Piran 2003).

($\sim \beta_f$) of the total energy, while most of the energy is in the internal energy of the shocked ejecta ($E_{\text{int}} \approx E \approx \Gamma_0 M_0 c^2$).¹² The relativistically hot shocked ejecta can then convert most of its internal energy back into kinetic energy through PdV work as the merged shell keeps expanding. This might initially (soon after the collision) accelerate the shell, and later cause it to decelerate more slowly with time (and radius), thus increasing the radius, R_{dec} , where it decelerates significantly from $R_{\text{dec}} \sim 2^{1/3} R_{\text{col}}$, where $R_{\text{col}} = R(t_{\text{col}}) = v_0 t_{\text{col}}$. However, even if all the original energy is back in the form of kinetic energy at R_{dec} , then still $E/c^2 \approx M_{\text{dec}} \beta_{\text{dec}}^2 \approx \beta_f M_{\text{sh}}$ where $\beta_{\text{dec}} = \beta(R_{\text{dec}}) \approx 0.4 d_{15} \gtrsim \beta_f$, $M_{\text{sh}} \approx (4\pi/3) \rho_{\text{ext}} R_{\text{col}}^3$ (Wilkin 1996) and $M_{\text{dec}} = M_{\text{ext}}(R_{\text{dec}}) \approx (4\pi/3) \rho_{\text{ext}} R_{\text{dec}}^3$. This gives

$$\frac{M_{\text{dec}}}{M_{\text{sh}}} \approx \left(\frac{R_{\text{dec}}}{R_{\text{col}}}\right)^3 \approx \frac{\beta_f}{\beta_{\text{dec}}^2} \lesssim \beta_{\text{dec}}^{-1} \sim 2.5 d_{15}^{-1}. \quad (2)$$

The angular diameter of the source at the time of the first observation, $t_1 \approx 7$ days, and at the epoch of deceleration, $t_{\text{dec}} \sim t_p \approx 33$ days, was $80\theta_{80}$ mas and $300\theta_{300}$ mas, respectively.¹³ The corresponding radii are $R_1 = 9.0 \times 10^{15} \theta_{80} d_{15}$ cm and $R_{\text{dec}} \approx 3.4 \times 10^{16} \theta_{300} d_{15}$ cm. The requirement that $R_{\text{col}} < R_1$ gives $R_{\text{dec}}/R_{\text{col}} \gtrsim 3.75$ and therefore $(R_{\text{dec}}/R_{\text{col}})^3 \approx 50(R_1/R_{\text{col}}) \gtrsim 50$, which is in contradiction with Eq. 2. This suggests that the simple model of a collision between the ejecta and an external shell fails to reproduce the observations if the outflow was initially relativistic ($\Gamma_0 \gg 1$). This is because, contrary to observations, R_{dec} would not be much larger than R_{col} , and instead $R_{\text{dec}}/R_{\text{col}} \lesssim 1.4 d_{15}^{-1/3}$.¹⁴

2.2. Newtonian Outflow

For a Newtonian outflow ($\beta_0 \ll 1$), Eq. 1 reduces to $\beta_f/\beta_0 \approx M_0/M_f$ where $M_f \approx M_0 + M_{\text{sh}}$. Since $M(R_{\text{col}} < r < R_{\text{dec}}) \sim M_f$ and $M_{\text{sh}} \approx (4\pi/3) \rho_{\text{ext}} R_{\text{col}}^3$, then $M_{\text{sh}} > M_0$ would imply $R_{\text{dec}}/R_{\text{col}} \sim 2^{1/3} \approx 1.26$, in contrast with observations.

Therefore, we must have $M_0 \gg M_{\text{sh}}$, which results in $\beta_f \approx \beta_0$, $M_f \approx M_0 \sim M_{\text{dec}} \approx (4\pi/3) \rho_{\text{ext}} R_{\text{dec}}^3$, and $M_0/M_{\text{sh}} \approx (R_{\text{dec}}/R_{\text{col}})^3 \gtrsim 50$. If the collision occurred at $t_{\text{col}} = 5t_{\text{col},5}$ days, then $R_{\text{col}} \approx (5t_{\text{col},5}/7) R_1 \approx 6.4 \times 10^{15} t_{\text{col},5} \theta_{80} d_{15}$ cm and $M_0/M_{\text{sh}} \approx (R_{\text{dec}}/R_{\text{col}})^3 \sim 140 t_{\text{col},5}^{-3}$. The observed source size implies $\beta_0 \approx \beta_f \approx R_{\text{dec}}/ct_{\text{dec}} \approx 0.4 d_{15}$. As the shocked external medium has comparable internal and kinetic energies, t_{dec} occurs when $E \approx (4\pi/3) \rho_{\text{ext}} R_{\text{dec}}^3 v_0^2 \approx 3.8 \times 10^{46} n_0 d_{15}^5$ erg, where $n_{\text{ext}} = \rho_{\text{ext}}/m_p = n_0 \text{ cm}^{-3}$. Thus $n_0 \approx 0.26 d_{15}^{-5} E_{46}$ and $M_0 \approx 2E/v_0^2 \approx 1.4 \times 10^{26} d_{15}^2 E_{46}$ g. These results for E and M_0 are similar to those derived by Gelfand et al. (2005).

Finally, it is important to keep in mind that the outflow might consist of more than one component. The simplest example is a relativistic shell (with $\Gamma \gg 1$) followed by a Newtonian shell that was ejected slightly later during the GF. The relativistic shell is shocked and decelerated to a Newtonian

¹² This result is valid when the ejecta shell collides with a dense and thin external shell (of width $\Delta R \ll R$), and is very different from the situation where the same ejecta gradually sweeps up the external medium over a large range in radii.

¹³ At t_1 the image is somewhat elongated and the quoted value is along the semi-major axis (?).

¹⁴ If the external density varied smoothly, with no sharp feature like a thin dense shell as in our basic scenario, then by the time of the first observation, when the expansion velocity is only mildly relativistic, the expansion would already be in the decelerating phase, and no coasting phase would have been observed.

velocity as it collides with the external shell, at $t_{\text{col},1}$, while the Newtonian shell catches up and collides with the slower merged relativistic + external shell at $t_{\text{col},2} > t_{\text{col},1}$. As long as the velocity after the first collision is sufficiently smaller than that of the Newtonian shell, the subsequent dynamics would not be very different than for the Newtonian outflow case discussed above. An important difference, however, is that the emission would light up at $\sim t_{\text{col},1}/2\Gamma^2 \ll t_{\text{col},2}$, i.e. much earlier than without the relativistic component.¹⁵ Rapid follow-up observations of future GFs could test this directly, and teach us more about the properties of the outflow. In the present case, the later collision with the Newtonian shell might explain the change in the degree of linear polarization (from decreasing to increasing with time) and its position angle, at $t \approx 10$ days (Gaensler et al. 2005).

We tested our basic scenario with the aid of numerical simulations (see Fig 1). Our basic picture is confirmed by these calculations, and the observed evolution of the source size is nicely reproduced. In a future work (Ramirez-Ruiz et al. 2005, in preparation) we investigate the dynamics in more detail, including the implications of aspherical outflows, which are relevant given the elongated nature of the radio image (Gaensler et al. 2005).

3. EXPLAINING THE OBSERVED RADIO EMISSION

Once the reverse shock crosses the ejecta and the forward shock crosses the bow shock shell, there is no more supply of newly accelerated electrons, and the existing relativistic electrons cool adiabatically as the shells expand, $\gamma_e \propto V^{-1/3}$, where $V = 4\pi R^2 \Delta R$ is the volume of the shell. At this stage, the observed radio flux decreases as $t^{-2.7}$, which may be explained within the scope of the toy model, initially outlined by Gaensler et al. (2005). If the expansion in the radial direction is small compared to that in the transverse directions ($\Delta R \approx \text{const}$) then $V \propto R^2 \propto t^2$. If in addition the magnetic field is mainly in the transverse direction then $B \propto V^{-1/2} \propto t^{-1}$. The spectral slope in the radio, of $F_\nu \propto \nu^\alpha t^\delta$ with $\alpha = -0.75 \pm 0.02$ (Gaensler et al. 2005) suggests that the radio band is in the frequency range $\nu_m < \nu_{\text{rad}} < \nu_c$ (this is verified for our model below) where $\alpha = (1-p)/2$, and therefore $p = 2.50 \pm 0.04$. In this frequency range $F_\nu = F_{\nu,\text{max}}(\nu/\nu_m)^{(1-p)/2}$, where $F_{\nu,\text{max}} \propto N_e B$ and $\nu_m \propto B\gamma_m^2$. Here N_e is the number of relativistic electrons that are emitting the synchrotron radiation, which is constant at this stage, so that $F_\nu \propto B^{(p+1)/2} \gamma_m^{p-1} \propto t^{(1-7p)/6}$ and $\delta = (1-7p)/6 = (7\alpha-3)/3 = -2.75 \pm 0.05$, in good agreement with the observed value of $\delta \approx -2.7$ (Gaensler et al. 2005). When the rebrightening bump is subtracted, the best fit to the power law is somewhat steeper (Gelfand et al. 2005) and such steepening can be attributed a somewhat tangled magnetic field geometry (Gaensler et al. 2005). However, the chief uncertainty here is the assumption that the shell maintains constant thickness.

The emission from the forward shock is dominated by the newly shocked electrons which are accelerated to relativistic energies with a power law distribution, $dN/d\gamma_e \propto \gamma_e^{-p}$ for $\gamma_e > \gamma_m$. At $t < t_{\text{dec}}$ the relative velocity of the shocked downstream fluid and the upstream fluid is roughly constant and equal to $v_{\text{rel}} = \beta_{\text{rel}}c \approx 0.3d_{15}c$ since $v_{\text{ref}}/v_0 \approx 3/4$. Let us define

$$\gamma_m^* = \frac{\epsilon_e}{\xi_e} \left(\frac{p-2}{p-1} \right) \frac{m_p}{m_e} \frac{\beta_{\text{rel}}^2}{2} = 2g\epsilon_{e,-1} \left(\frac{\beta_{\text{rel}}}{0.26} \right)^2, \quad (3)$$

where $g = 3(p-2)/(p-1)$ ($= 1$ for $p = 2.5$), $\epsilon_e = 0.1\epsilon_{e,-1}$ (ϵ_B) is the fraction of the post shock internal energy density in relativistic electrons (magnetic fields), and ξ_e is the fraction of electrons that are accelerated to relativistic energies.

We have $\gamma_m \approx \max(2, \gamma_m^*)$, since for $\gamma_e < 2$ the electrons are no longer relativistic. Gelfand et al. (2005) calculate the light curve under the assumption that $\epsilon_e/\xi_e = \text{const}$ and $\gamma_m^* > 2$ (see Frail, Waxman & Kulkarni 2000), which is valid for $\epsilon_e > 0.1$ or $\xi_e \ll 1$ until there is significant deceleration. Once $\gamma_m^* < 2$, the behavior of ϵ_e and ξ_e depends on poorly understood shock acceleration of non-relativistic electrons. Here it is assumed that $\xi_e \approx \min(1, \gamma_m^*/\gamma_m)$ which is equivalent to the assumption of a constant ϵ_e . Eq. 3 shows that for $\epsilon_{e,-1} \lesssim 1$ (and it is difficult for ϵ_e to be much higher than 0.1) we have $\gamma_m \lesssim 2$ all along, so that $\gamma_m \approx 2$ is constant, while $\xi_e \sim \gamma_m^*/2$ decreases with time at $t \gtrsim t_{\text{dec}}$.

Now, $v_{\text{rel}}/v_0 \approx (t_{\text{dec}}/t)R_{\text{sh}}/R_{\text{dec}} \approx \min[1, (t/t_{\text{dec}})^{-3/5}]$ where $t_{\text{dec}} = R_{\text{dec}}/v_{\text{sh},0} = (3E/2\pi\rho_{\text{ext}}v_{\text{sh},0}^5)^{1/3}$ and $v_{\text{sh},0} = v_f(\hat{\gamma}+1)/2 \approx v_0(\hat{\gamma}+1)/2$ where $\hat{\gamma} = 5/3$ is the adiabatic index. At $t \gg t_{\text{dec}}$ the shock approaches the Sedov-Taylor self similar solution, where $R_{\text{sh}} = \xi(Et^2/\rho_{\text{ext}})^{1/5}$ with $\xi \approx 1$. The post shock magnetic field is $B = (8\pi\epsilon_B e_{\text{int}})^{1/2}$ where $e_{\text{int}} = \rho_{\text{ext}}v_{\text{rel}}^2(\hat{\gamma}+1)/2(\hat{\gamma}-1)$. We have $N_e = \xi_e M/m_p$ where $M = f_b(4\pi/3)\rho_{\text{ext}}R_{\text{sh}}^3$ and f_b is the beaming factor (i.e. the fraction of the total solid angle occupied by the flow). Also $L_{\nu,\text{max}} = P_{\nu,\text{max}}N_e$ where $P_{\nu,\text{max}} \approx P_{\text{syn}}/\nu_{\text{syn}}$, $P_{\text{syn}}(\gamma_e) = (4/3)\sigma_{\text{TC}}(B^2/8\pi)\gamma_e^2$ and $\nu_{\text{syn}}(\gamma_e) = eB\gamma_e^2/2\pi m_e c$. What is more, $\nu_m = \nu_{\text{syn}}(\gamma_m)$ and $F_{\nu,\text{max}} = L_{\nu,\text{max}}/4\pi d^2$. Thus at $t > t_{\text{dec}}$ we have

$$F_\nu = 4.2 f_b g n_0^{3(p+1)/20} E_{46}^{(11+p)/10} \epsilon_{e,-1} \left(\frac{\epsilon_B}{0.002} \right)^{(p+1)/4} d_{15}^{-2} \\ \times \left(\frac{\nu}{8.5 \text{ GHz}} \right)^{(1-p)/2} \left(\frac{t}{33 \text{ days}} \right)^{-3(p+1)/10} \text{ mJy}, \quad (4)$$

where the value of the numerical coefficient is for $p = 2.5$, while $F_\nu(t < t_{\text{dec}}) \approx (t/t_{\text{dec}})^3 F_\nu(t_{\text{dec}})$.

The parameter values in Eq. 4 were chosen to match the observed flux at the peak of the rebrightening, $t_{\text{dec}} \approx t_p \approx 33$ days. This demonstrates that an energy of $\sim 10^{46}$ erg, comparable to that in the GF (if it was emitted roughly isotropically), can be accommodated for reasonable values of the micro-physical parameters and the external density. Taking into account the relation $n_0 \approx 0.26d_{15}^{-5}E_{46}$ derived in §2.2, we find that an equipartition limit $\epsilon_e, \epsilon_B \lesssim 0.3$ (0.5) gives $E_{44} \gtrsim 7.5d_{15}^{1.9}$ ($4.0d_{15}^{1.9}$), consistent with the conclusions of Gelfand et al. (2005).

Finally, we estimate the expected flux at the end of the collision between the ejecta and the external shell, $\sim t_{\text{col}}$. The external shell is accelerated to $\beta_f \approx \beta_0$ while the ejecta is only slightly decelerated, so that the shock going into the external shell is stronger and likely to dominate the emission. The volume of the shell, $4\pi\eta R_{\text{col}}^3$ where $\eta = \Delta R/R_{\text{col}} = 0.1\eta_{-1}$, is reduced by a factor of 4 due to shock compression, and its internal energy is a fraction $M_{\text{sh}}/M_f \approx M_{\text{sh}}/M_0 \approx 0.007t_{\text{col},5}^3$ of the total energy E . Under similar assumptions as above,

¹⁵ A similar result is obtained also if there is a continuous external medium instead of a shell surrounding a cavity.

$$F_\nu(t_{\text{col}}) \approx 80 f_b g^{p-1} \eta_{-1}^{-(p+1)/4} E_{46}^{(5+p)/4} \epsilon_{e,-1}^{p-1} \epsilon_{B,-1}^{(p+1)/4} \times d_{15}^{(5p-27)/4} \left(\frac{\nu}{8.5 \text{ GHz}} \right)^{(1-p)/2} t_{\text{col},5}^3 \text{ mJy}, \quad (5)$$

in rough agreement with the extrapolation to $t_{\text{col}} \sim 5$ days of the observed flux, $F_{\nu=8.5 \text{ GHz}} = 53 \text{ mJy}$, at the first epoch, $t = 6.9$ days (Cameron & Kulkarni 2005; Gaensler et al. 2005).

For the parameter values used in Eq. 5 we obtain $\nu_m \sim 1 \text{ MHz}$, $\nu_{\text{sa}} \sim 50 \text{ MHz}$ and $\nu_c \sim 10^{17} \text{ Hz}$ at $t_{\text{col}} \sim 5$ days, so that the radio frequencies are well within the assumed power law segment of the spectrum. Soon after the shock finishes crossing the shell, the electron power law energy distribution extends up to $\gamma_{\text{max}} \sim \gamma_c(t_{\text{col}}) \sim 10^6$. Thereafter adiabatic cooling takes over and $\gamma_{\text{max}} \propto t^{-2/3}$, while $B \propto t^{-1}$ so that $\nu_{\text{syn}}(\gamma_{\text{max}}) \sim \nu_c(t_{\text{col}})(t/t_{\text{col}})^{-7/3}$. The emission from the shocked external medium starts to dominate at $t \approx 25$ days, i.e. $t/t_{\text{col}} \sim 5$, and hence at that time $\nu_{\text{syn}}(\gamma_{\text{max}}) \gtrsim 10^{15} \text{ Hz}$ is well above the radio.

4. DISCUSSION

We have described a dynamical model for the interaction with the surrounding medium of the outflow that was ejected during the 2004 Dec. 27 giant flare (GF) from SGR 1806-20. This model reasonably accounts for the evolution of the source size with time as well as for the observed radio light curves and spectrum. Using a simple analytic model, we have shown that the outflow from the GF could not have been highly relativistic, and was instead only mildly relativistic,¹⁶ with an average velocity of $v \sim 0.4d_{15}c$, similar to the observed roughly constant expansion velocity over the first month or so. The local expansion velocity is slightly higher along the elongated direction of the image, which has an axis ratio of ~ 1.7 (Gaensler et al. 2005). This sets a lower limit on the true axis ratio of the emitting region, due to projection effects, suggesting a relatively mild collimation of the outflow into a wide jet. Still, even the maximal local expansion velocity was only mildly (rather than highly) relativistic.

Lower limits on the energy, $E \gtrsim 10^{44.5} \text{ erg}$, and mass, $M_0 \gtrsim 10^{24.5} \text{ g}$, of the outflow, and on the external den-

sity, $n_{\text{ext}} \gtrsim 10^{-2} \text{ cm}^{-3}$ have been derived by citet[[see also §3]Gelfand05]. The values of E , M_0 and n_{ext} scale linearly with each other. The bow shock stand-off radius is $R_{\text{bs}} = 6.4 \times 10^{15} L_{34.5}^{1/2} n_0^{-1/2} v_{350}^{-1} \text{ cm}$, where $v_* = 350 v_{350} \text{ km s}^{-1}$ is the velocity of SGR 1806-20 relative to the ISM, and $L = 10^{34.5} L_{34.5} \text{ erg s}^{-1}$ is its spin-down luminosity.¹⁷ In our scenario, $R_{\text{col}} \approx 6.4 \times 10^{15} t_{\text{col},5} d_{15} \text{ cm}$ is $\sim R_{\text{bs}}$, which is indeed the case for the above parameter values. Note, however, that $E \sim 10^{46.5} n_0 \text{ erg}$ and $M_0 \sim 10^{26.5} n_0 \text{ g}$, while the minimal allowed density, $n_0 \sim 10^{-2}$, requires $v_* \sim 3500 \text{ km s}^{-1}$ and a similar kick velocity for SGR 1806-20 at its birth, which is extremely high. This suggests that the true values of E , M_0 and n_{ext} are larger than their lower limits by a factor of $\sim 100 n_0 \sim 100 v_{350}^{-2}$.

A much dimmer radio afterglow was detected following the 1998 Aug. 27 GF from SGR 1900+14 (Frail, Kulkarni & Bloom 1999), which despite the much sparser data, shows similarities to the radio afterglow discussed here. This suggests that our model might be applicable more generally. The spin down luminosity L of the two SGRs is comparable, and so is the time at which the light curve decays steeply ($\sim 9-10$ days), suggesting that R_{bs} in each case is not very different. This would imply a similar $n_{\text{ext}} v_*^2$. Under these assumptions, the large difference in the radio luminosity (by a factor of ~ 500) would be mainly a result of the much larger energy content carried by the outflow of SGR 1806-20 immediately after the GF.

This research was supported by US Department of Energy under contract number DE-AC03-76SF00515 (J.G.) and by NASA through a Chandra Postdoctoral Fellowship award PF3-40028 (E. R.-R.). The software used in this work was in part developed by the DOE-supported ASCI/Alliance Center for Astrophysical Thermonuclear Flashes at the University of Chicago. Computations were performed on the IAS Scheide computer cluster. B.M.G. and J.D.G. were supported by NASA through LTSA grant NAG5-13032. The National Radio Astronomy Observatory is a facility of the National Science Foundation operated under cooperative agreement by Associated Universities, Inc.

¹⁶ This refers to the ejecta which carried most of the energy in the outflow. A small fraction of the energy might still have been carried by highly relativistic outflow.

¹⁷ Before 1999 $L_{34} \approx 0.8$ while by 2001 and until before the Dec. 27th GF it leveled off at $L_{34} \approx 4.5$ (Woods et al. 2005, in preparation). The dynamical timescale for the bow shock is $t_{\text{bs}} \sim R_{\text{bs}}/v_* = 10 L_{44} n_0^{-1/2} v_{200}^{-2} \text{ yr}$. In our scenario, $R_{\text{bs}} \sim R_{\text{col}}$ so that $t_{\text{bs}} \sim 10 t_{\text{col},5} d_{15} v_{200}^{-1} \text{ yr}$. Since the spin

down rate of SGR 1806-20 increased by a factor of ~ 5 several years before the GF, the steady state assumption for the bow shock is not valid for $v_{200} \lesssim 3$. As a rough guide, one might still use the results for a steady wind (Wilkin 1996), with the average spin down luminosity over a period t_{bs} . The exact shape of the bow shock could, however, be different than that of a steady wind.

REFERENCES

- Cameron, P. B., & Kulkarni, S. R. 2005, GCN Circ., 2928
 Corbel, S., & Eikenberry, S. S. 2004, A&A, 419, 191
 Duncan, R. C., & Thompson, C. 1992, ApJ, 392, L9
 Frail, D. A., Kulkarni, S. R., & Bloom, J. S. 1999, Nature, 398, 127
 Frail, D. A., Waxman, E., & Kulkarni, S. R. 2000, ApJ, 537, 191
 Gaensler, B. M., et al. 2005, Nature in press (astro-ph/0502393)
 Gelfand, J. D., et al. 2005, submitted to ApJL (astro-ph/0503269)
 Granot, J., Nakar, E., & Piran, T. 2003, Nature, 426, 138
 Hurley, K., et al. 2005, submitted to Nature (astro-ph/0502329)
 Kouveliotou, C., et al. 1998, Nature, 393, 235
 Palmer, D. A., et al. 2005, Nature in press (astro-ph/0503030)
 Wilkin, F. P. 1996, ApJ, 459, L31

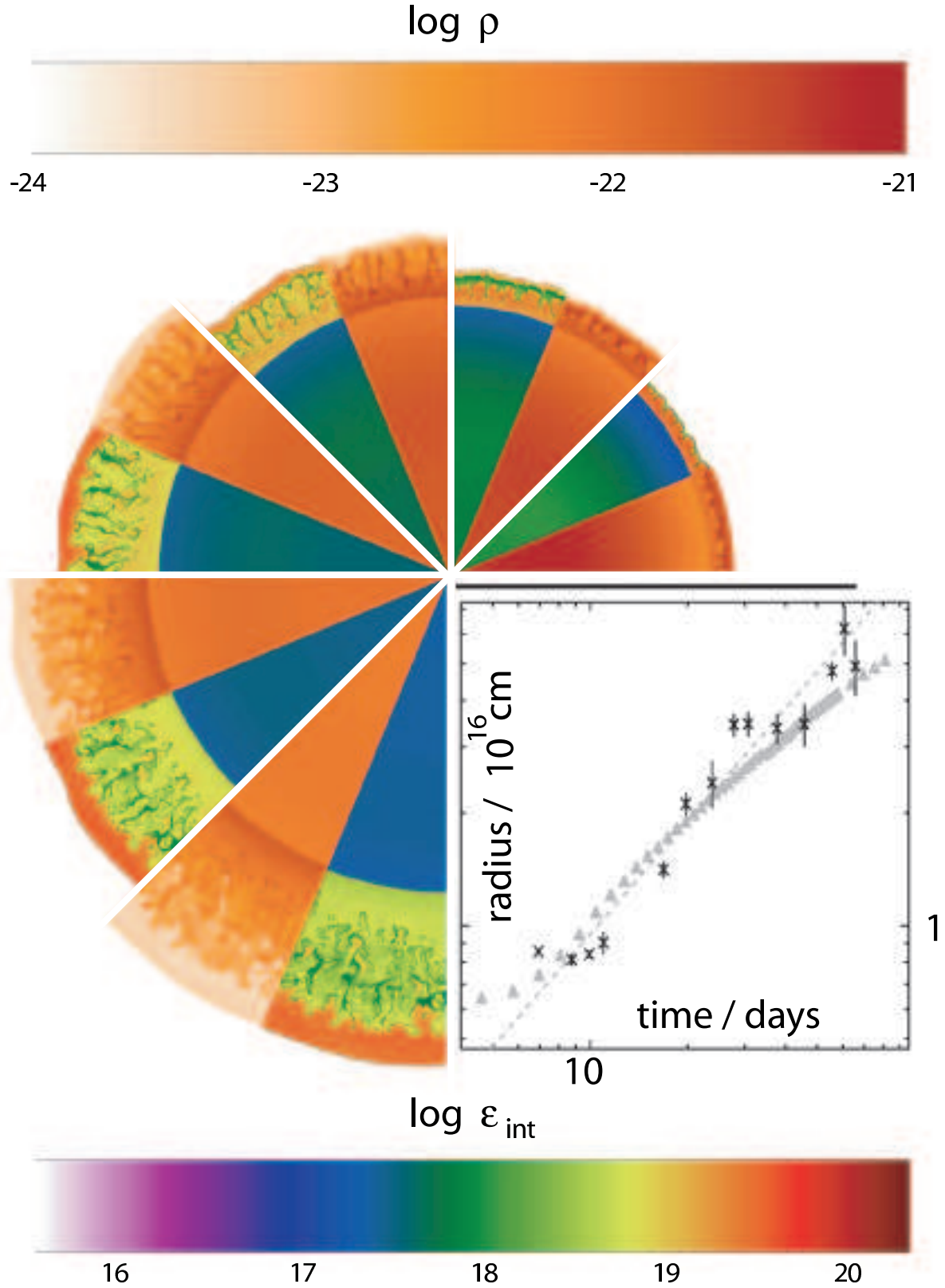


FIG. 1.— Numerical simulation of the collision between the outflow ejected during the SGR giant flare and a pre-existing cavity. The evolution of the density (ρ in g/cm^3) and specific internal energy (ϵ_{int} in erg/g) are shown. Calculations were done in two dimensions using the FLASH code. The initial configuration is as follows. In the inner region (outflow from the SGR, inner 5×10^{14} cm) both a thermal energy of 10^{46} erg and ejecta mass, M_0 , are distributed uniformly; M_0 is selected so that $v = (2E/M_0)^{1/2} \approx 0.4c$. The injected gas and surrounding ISM (with $\rho_{\text{ext}} = 2 \times 10^{-24}$ g/cm^3) are characterized by a 5/3 adiabatic index. More details will be presented in Ramirez-Ruiz et al. (2005, in preparation). The black horizontal line in the figure corresponds to a scale of 10^{16} cm. Anti-clockwise, from right, the slices are for $t = 5.79, 6.95, 8.11, 9.26, 10.42, 11.58$ days. *Inset Panel:* Temporal evolution of the observed size of the simulated source, together with the radio measurements of Taylor et al. (in preparation).